Adoption of CO_2 blended with C_6F_6 as working fluid in CSP plants

Cite as: AIP Conference Proceedings **2445**, 090005 (2022); https://doi.org/10.1063/5.0086520
Published Online: 12 May 2022

Giampaolo Manzolini, Marco Binotti, Ettore Morosini, et al.

Adoption of CO_2 Blended with C_6F_6 as Working Fluid in CSP Plants

Giampaolo Manzolini[1,a)], Marco Binotti[1], Ettore Morosini[1], David Sanchez[2], Francesco Crespi[2], Gioele Di Marcoberdino[3], Paolo Iora[3] and Costante Invernizzi[3]

[1]*Politecnico di Milano, Dipartimento di Energia, Via Lambruschini 4, 20156 Milano, Italy*
[2]*Universidad de Seville, Camino de los descubrimientos s/n, 41092 Seville, Spain*
[3]*Università degli Studi di Brescia, via Branze, Brescia Italy*

[a)]Corresponding author: giampaolo.manzolini@polimi.it

Abstract. The adoption of CO_2-based mixtures as power block working fluid for CSP plant can turn supercritical CO_2 cycles into efficient transcritical cycles even at high ambient temperature, with significant performance improvement and potential power block cost reduction. In this work, the use of CO_2+C_6F_6 mixture as working fluid for a power cycle coupled with a solar tower is analyzed. Two different cycle maximum temperatures (550°C and 650°C) are considered and for both configurations the overall plant design is performed. The yearly energy yield is computed with hourly data and the LCOE is minimized varying storage and cycle recuperator sizes. Results show comparable results for the innovative working fluid and for the sCO_2 cycles.

INTRODUCTION

Today, most of the CSP plants worldwide use conventional steam Rankine cycles for the conversion of thermal power into electricity with advantages related to the use of a well-known technology and disadvantages related to the high capital cost and large turbomachinery. Recently, many efforts have been made towards innovative solutions in order to overcome some of the disadvantages: supercritical CO_2 closed cycles (sCO_2) are identified as one of the most promising technologies with several ongoing projects worldwide [1][2]. Nevertheless, the compression of pure CO_2 near the critical region presents some difficulties: designing an efficient compressor to work with a fluid whose behavior is so sensitive to its predicted operating conditions is challenging. Operation-wise, the variability of fluid properties leads to difficulties in operating the system at off-design. When no low-temperature coolant (below 20°C) is available for the cycle heat rejection, the compressor operates well above the CO_2 critical point (T_{crit}=31°C), limiting the real gas effect and the advantages in terms of compression work: this condition is typical of hot environments, and characteristic of CSP applications.

A promising solution for reducing the compression work and avoiding the abovementioned design and operation hurdles, is the replacement of the compression in supercritical conditions with a pump in the liquid region: this would require a working fluid with critical temperature higher than 70 °C and limited critical pressure; this latter feature would enable to exploit higher compression ratios keeping the same advantages over steam Rankine cycles as of pure CO_2, as the cycle compactness. CO_2-based mixtures can be a solution for these applications: mixing the CO_2 with certain dopants with high critical temperature rises the overall mixture critical temperature, yielding a more suitable working fluid for transcritical closed cycles in CSP applications.

This work focuses on the adoption of CO_2 blended with C_6F_6 as working fluid for CSP applications characterized by different maximum temperatures (550°C and 650°C): this work is part of the EU funded SCARABEUS project [3], which aims at demonstrating the technical feasibility of the use of innovative CO_2-based binary mixtures, as working fluid for CSP cycles, in hot and arid environment characterized by high ambient temperatures.

SolarPACES 2020
AIP Conf. Proc. 2445, 090005-1–090005-9; https://doi.org/10.1063/5.0086520
Published by AIP Publishing. 978-0-7354-4195-8/$30.00

CO_2+C_6F_6 MIXTURE AS NOVEL WORKING FLUID IN TRANSCRITICAL CYCLES

The proper CO_2-based mixture identified as novel working fluid must have a critical temperature significantly higher than the one of pure CO_2, in order to guarantee a liquid phase flow during all the compression phase (i.e. both at pump inlet and outlet). C_6F_6 is characterized by a high critical temperature (243°C), low critical pressure (32.8 bar) and low toxicity: for these reasons it was selected as potential candidate for CO_2-blending. A set of experimental bubble points for the CO_2-C_6F_6 mixture, available in literature in the 20°C-80°C temperature range [4], is used to fit the binary interaction parameters (BIP) of two different cubic Equations of State (EoS): the standard Peng-Robinson (PR) and the Peng Robinson with Boston-Mathias alpha function (PR-BM). The two equations of state are modelled in ASPEN Plus® v.10 [5].

The BIP that best fit the experimental data are $k_{ij} = 0.033$ and $k_{ij} = 0.038$ for PR and PR-BM, respectively. The good agreement of the two EoS with the experimental bubble point in [4] for a CO_2 molar fraction of 85% is shown in Figure 1 (a). The identification of the optimal molar fraction of C_6F_6 is based on a preliminary evaluation of the cycle efficiency of a simple-recuperative cycle, assuming a maximum temperature of 550°C and considering the assumptions reported in Table 1. Figure 1 (b), reports the trends of the gross cycle efficiency for both EoS: considering these calculations, the molar compositions is set at 84% CO_2, which is close to the maximum cycle efficiency for both EoS.

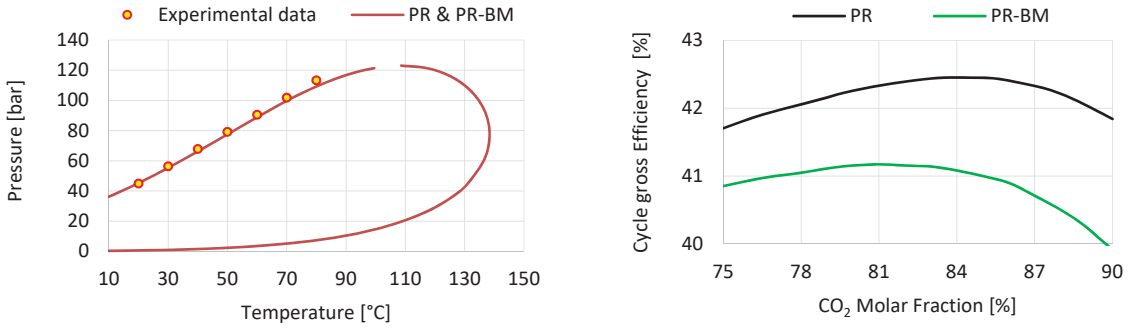

(a) (b)

FIGURE 1. (a) Results of the BIP optimization of both PR and PR-BM on the experimental bubble points for the mixture at $x_{CO2} = 85\%$ as the closest experimental composition available to the one selected (b) Gross cycle efficiency of the simple recuperative cycle described in Table 1 at $T_{max} = 550$°C, for various molar fractions

METHODOLOGY

The performances of the cycle exploiting the novel working fluid are estimated with Aspen Plus at two temperature levels (550°C and 650°C). The obtained temperatures at the inlet/outlet of the primary heat exchanger are then adopted to size two different solar tower plants: a medium temperature solution using solar salts as HTF and a high temperature solution using liquid sodium as HTF. Both plants include a two-tank direct thermal energy storage (TES) system. The yearly analysis is performed using hourly weather data. The adopted procedure for the plant design, the calculation of its thermodynamic and cost performance and the software used are depicted in Figure 2 (a), while a schematic of the ST plants is reported in Figure 2 (b). Results are compared with pure CO_2 or steam to outline the potential advantages of the proposed technology.

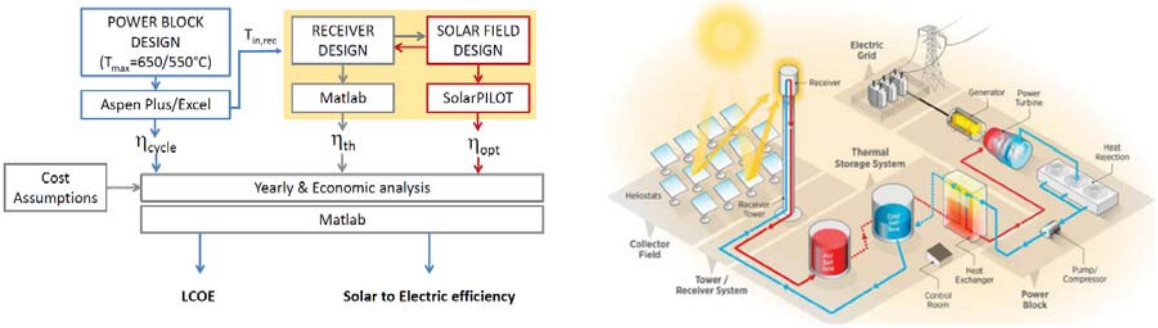

(a) (b)

FIGURE 2. Schematic of the methodology adopted for the sCO_2 and the CO_2+C_6F_6 cycles (a) and system layout [6] (b)

Power Block Design

Once the working fluid is defined, the plant layout and the cycle assumptions play the most important role in the techno-economic analysis of the cycle. The CO_2-C_6F_6 mixture is characterized by a higher molecular complexity than pure CO_2 and it is thus characterized by a limited variation of C_P in the considered pressure and temperature ranges. Due to this characteristic, a single recuperator can be sufficient to reach high cycle efficiencies since the average temperature difference between the high and low pressure sides can be kept lower than the one of sCO_2 at the same conditions. A simple transcritical recuperative cycle is hence considered (see Figure 3 (a)). The main assumptions for the power block simulation are listed in Table 1, while Figure 3 (b) reports the cycle T-s diagram for the selected composition and for the PR EoS: it is possible to notice the critical temperature at about 110°C and the overall compression phase in the liquid region, below the critical temperature.

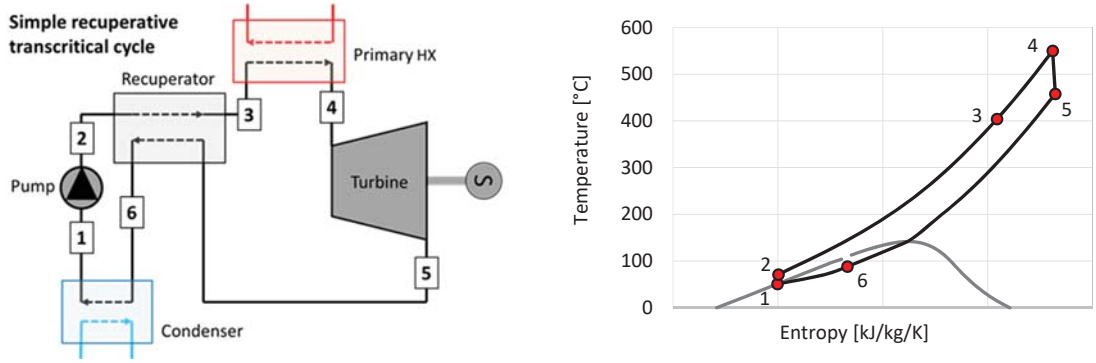

(a) (b)

FIGURE 3. Power block layout of the simple recuperative transcritical cycle (a). T-s diagram of the selected mixture at $x_{CO2} = 84\%$ for the PR EoS (b)

TABLE 1. Main assumptions for the power cycle simulation both at 650°C and 550°C

Parameter	Value	Parameter	Value
Pump outlet pressure (bar)	257.5	Δp heat rejection Heat Exchanger (bar)	2
Minimum temperature (°C)	51	Compressor/Pump isentropic efficiency	0.88
Δp HP/LP side of regenerator (bar)	0.5/1	Turbine isentropic efficiency	0.919
Δp Primary Heat Exchanger (bar)	4	Mechanical/Electrical efficiency	0.99/0.99
ΔT HTF T_{MAX} / Cycle T_{MAX}	15°C	Electric consumption of the heat rejection system per unit of heat rejected	1.5%

The size of the recuperator, which directly determines the primary heat exchanger inlet temperature (point 3), is varied to identify the minimum LCOE in each considered configuration. The pump outlet pressure is set to $P_2 = 257.5\ bar$ to be consistent with the reference case with $P_{MAX} = 250 bar$ accounting for the overall pressure drops of $7.5\ bar$ along the heating and cooling phases.

The comparison with pure sCO_2 cycles is evaluated at the same conditions, assuming the same cost models and installation site. The recompressed recuperative cycle, which is identified as one of the best configurations for solarized CO_2 cycles [2], is selected as reference configuration for pure sCO_2, using the same assumptions of the transcritical cycle (see TABLE 1), where the same values of pressure drops in the PCHE of the simple recuperative cycle are assumed for both PCHEs in the recompressed cycle.

Solar Field Design and Thermal Energy Storage

The design of the two different solar fields using solar salts and sodium as HTF is carried out with SolarPilot, a tool for field design optimization [7]. The design of the solar tower using solar salts as HTF considers a receiver similar to the one of the Gemasolar plant, while for the high temperature sodium receiver a reduced size (50% with respect to solar salts) is assumed, thanks to the possibility of tolerating higher solar fluxes for this HTF [8]. The field layouts are designed assuming about 190 MW at the receiver surface and a solar multiple equal to 2. The other relevant characteristics of the two solar field are available in [9]. A thermal model developed in MATLAB is used to estimate the receiver convective and radiative loss and the receiver thermal efficiency at design and off design conditions [10] [11]. In Figure 4, the two receivers thermal efficiencies as function of the solar radiation on the receiver and of the inlet HTF temperature are reported for a fixed maximum temperature of 565°C and 665°C, respectively.

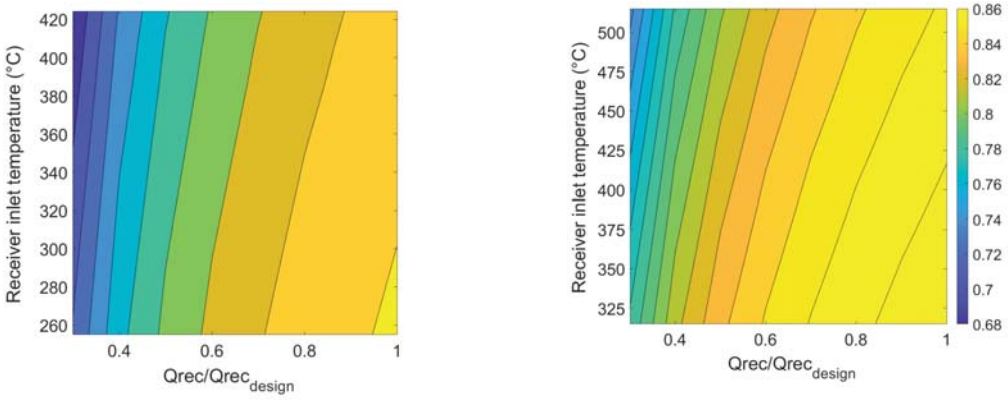

(a) (b)

FIGURE 4. Thermal efficiency of the receiver as function of the HTF inlet temperature and of the incoming solar radiation considering solar salts (a) and sodium (b) as heat transfer fluids

The two-tank direct TES system is designed considering the fluid volume and an additional 20% volume to account for the volume at the bottom of the tank required for pump suction head and the tank freeboard volume above the stored fluid with full storage [6]. For the sodium case, the hot tank storage operating at 665°C is designed assuming an internally insulated configuration, which uses refractory bricks in direct contact with the HTF to reduce the maximum temperature that the metal tank wall has to withstand [12]. The internal insulation allows to use lower-cost alloys, as the ones currently used for the hot solar salt storage tank operating at 565°C. The tank size is influenced by the power cycle temperature variation across the primary heat exchanger and is varied from 7 to 11 hours to maximize the economic performance of the plant.

Cost Model

The economic analysis of the power block for the transcritical cycles working with CO_2-C_6F_6 is based on correlations developed for sCO_2 cycles, since no cost models for these cycles are available in literature. They consider the compression step in supercritical conditions and therefore they do not fully implement the very advantage of transcritical cycles with respect to sCO_2. All the power block assumptions except for the PHE are taken from Weiland

et al [13], while the PHE cost model is taken from Carlson et al [14], since Weiland considered only gas-fired PHE that are not used in these applications.

The TES cost for the solar salts case is estimated assuming as reference costs the ones reported in [6] updated according to [15], while for the sodium case, the high temperature storage tank (i.e. 665°C) cost is corrected considering the extra cost for the internal insulation [12]. The solar field costs and receiver costs are taken from literature [6] [16]. Indirect and contingency costs are 20% of the total Capex. The LCOE is computed as follows, considering a capital recovery factor (CRF) of 9.37% that accounts for 8% discount rate:

$$LCOE\ \left[\frac{\$}{MWh}\right] = \frac{Total\ Plant\ CAPEX \cdot CRF + Fixed\ OPEX}{Yearly\ net\ Energy\ produced} + variable\ OPEX \tag{1}$$

RESULTS OF THE TECHNO-ECONOMIC ANALYSIS

The main technical and economic results are presented for all the four selected cases as function of the PCHE size represented by the parameter UA_{PCHE}/Q_{IN}. Table 2 summarizes the characteristics of the cycles that optimize the LCOE of the plant for each of the four configurations. The relation between the Minimal Internal Temperature Approach of the PCHE and the UA_{PCHE}/Q_{IN} of the transcritical cycle is presented in Figure 5. From the same figure it is possible to appreciate that the transcritical cycle power block specific Capex is about 5% lower than the supercritical one. In addition, it can be noted that the optimal transcritical cycle when integrated in the solar plant occurs for MITA around 5°C: a lower temperature difference in the recuperator increases the plant costs (in particular the PCHE) with limited advantages in terms of LCOE.

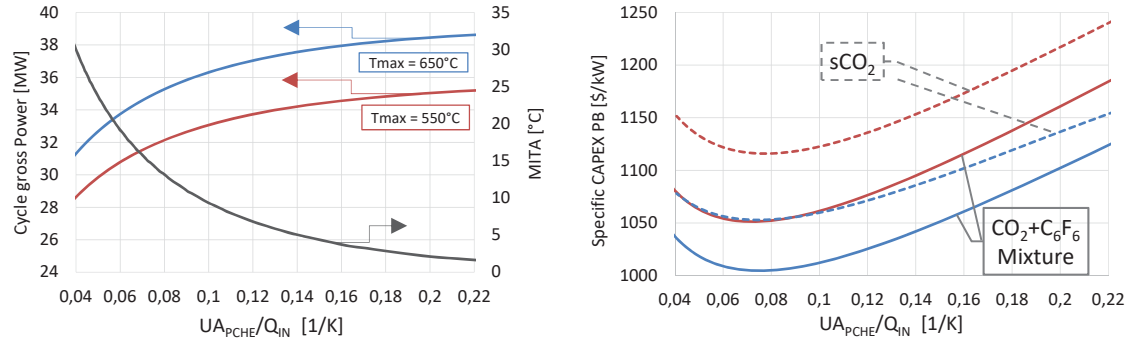

FIGURE 5. Cycle gross power and MITA for the CO_2+C_6F_6 cycle (a). Specific CAPEX of the power block for both the sCO_2 and the CO_2+C_6F_6 cycle (b) – Red curves: $T_{Max} = 550°C$. Blue curves: $T_{Max} = 650°C$

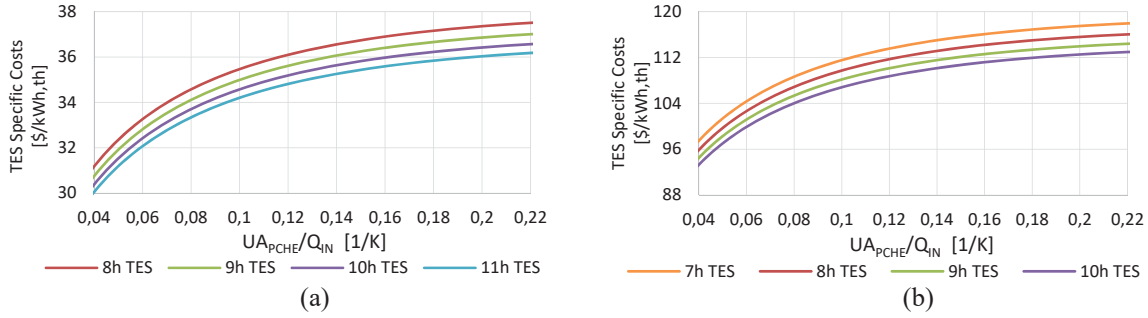

FIGURE 6. Specific TES costs for ST plants based on transcritical CO_2+C_6F_6 cycle, using Solar salts (a) or Sodium (b) as HTF and storage fluid.

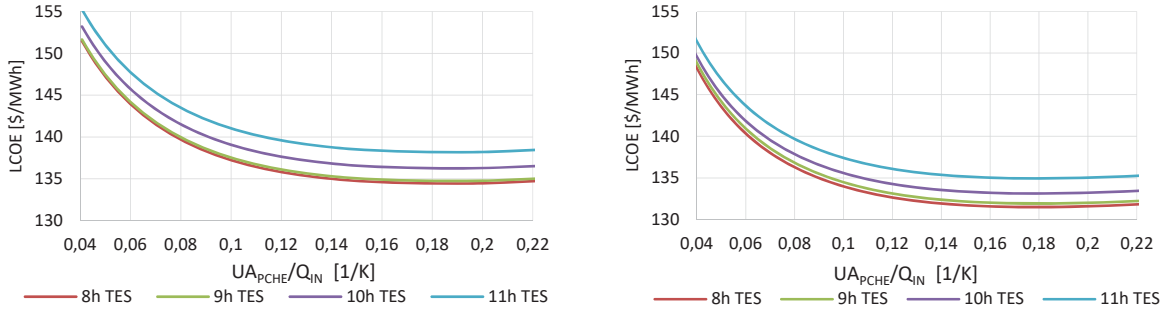

(a) (b)

FIGURE 7. LCOE of the cycles with $T_{MAX} = 550°C$ and solar salts as HTF - sCO2 (a). CO_2+C_6F_6 cycle (b)

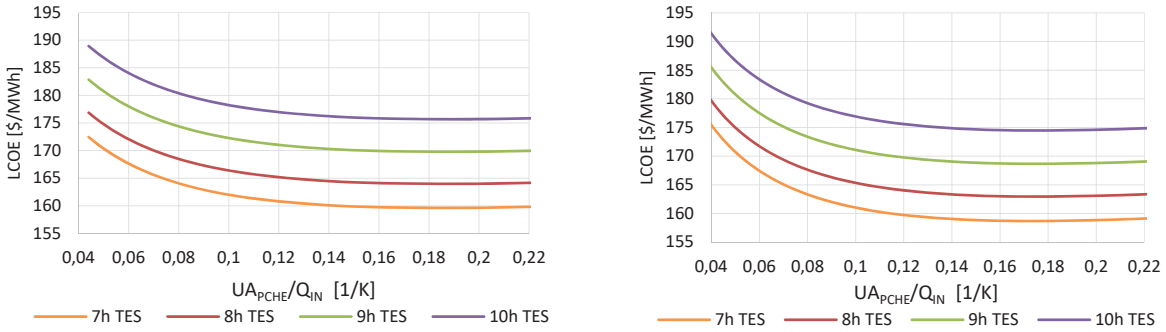

(a) (b)

FIGURE 8. LCOE of the cycles with $T_{MAX} = 650°C$ and sodium as HTF - sCO_2 (a). CO_2+C_6F_6 cycle (b)

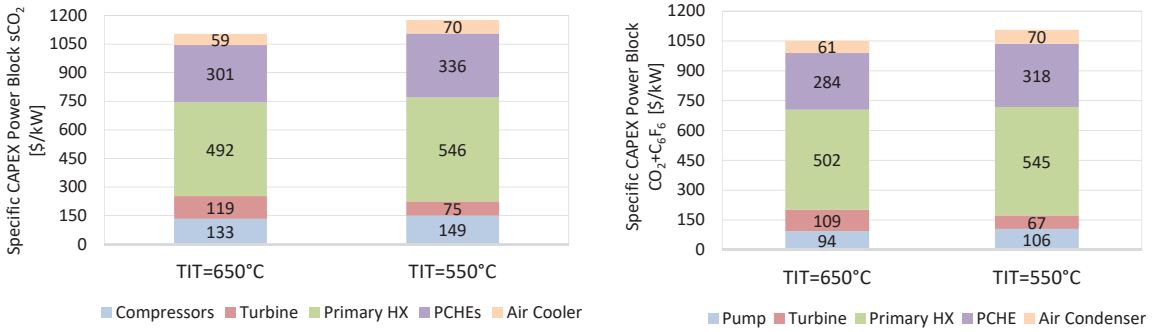

(a) (b)

FIGURE 9. Power Block specific CAPEX for optimal sCO_2 (a) and CO_2+C_6F_6 (b) cycles at T_{MAX} of 550°C and 650°C

TABLE 2. Thermodynamic and costs performances for the four investigated system layouts

	sCO_2 Tmax = 550°C	**sCO_2 Tmax = 650°C**	**CO_2+C_6F_6 Tmax = 550°C**	**CO_2+C_6F_6 Tmax = 650°C**
Equation of state	Span and Wagner	Span and Wagner	Peng Robinson	Peng Robinson
Minimum Pressure [bar]	105	105	77.6	77.6
Primary HX inlet Temperature [°C]	411	498	404	495
Mass flow rate [kg/s]	463	424	409	382
Compressors/Pump Power [MW]	10.0 (LT) / 7.7 (HT)	9.9 (LT) / 7.5 (HT)	8.1	7.6
Turbine Power [MW]	51.8	55.5	42.3	45.1
Cycle Gross Power [MW]	34.1	38.1	34.2	37.5
Condenser duty [MW]	46.3	42.8	46.0	43.4
Cycle Gross Efficiency [%]	42.42	47.10	42.50	46.37
Net Power-Block Power [MW]	32.7	36.7	32.8	36.1
Net Electric Power [MW]	31.7	35.4	31.8	34.8

	sCO_2 Tmax = 550°C	sCO_2 Tmax = 650°C	CO_2+C_6F_6 Tmax = 550°C	CO_2+C_6F_6 Tmax = 650°C
Receiver thermal efficiency [%]	84.95	86.22	85.0	86.24
TES Capacity [h]	8	7	8	7
UA_{PCHE}/Q_{IN} [1/K]	0.16	0.16	0.15	0.15
PHE UA [MW/K]	5.4	5.4	5.4	5.4
PCHEs UA [MW/K]	6.0 (HT) / 5.8 (LT)	6.8 (HT) / 5.2 (LT)	11.2	11.4
Specific costs PB [$/kW]	1176	1104	1106	1050
Heliostat field [M$]	40.8	42	40.8	42
Solar Tower + Receiver [M$]	52.7	46.2	52.7	46.2
Storage [M$]	25	67.2	23.5	65.1
Power Block [M$]	40.1	42.1	37.4	39.4
Indirect + Contingency Costs [M$]	31.8	39.6	30.9	38.5
Total CAPEX [M$]	190.6	237.1	185.3	231.2
Power Plant specific costs [$/$kW_{el}$]	6015	6698	5830	6645
Yearly Net Energy Produced [GWh]	149	154	149.4	151.6
Fixed OPEX [M$/year]	1.8	1.8	1.8	1.8
Variable OPEX [$/MWh]	3.5	3.5	3.5	3.5
Discount rate [%] - Plant lifetime [y]	8 - 25	8 - 25	8 - 25	8 - 25
Equivalent Hours [h/year]	4700	4322	4698	4325
Solar to Electric efficiency [%]	22.78	24.75	22.21	24.34
LCOE [$/MWh]	135	160	132	159

The higher LCOE for the high temperature ST plants is mainly due to the choice of a direct two-tank TES which implies the use of sodium also as storage fluid: the lower density and specific heat of sodium, together with its higher unit cost with respect to solar salts (2.00 $/kg vs 0.80 $/kg) implies higher TES cost (see Figure 6). The storage cost can be reduced using a single tank TES with thermocline and filler material [17] or by considering an indirect two-tank storage using high temperature chloride solar salts as storage fluid. The selected storage size for the high temperature ST plants is thus the minimum within the considered range (7h), while for the for solar salts configuration is 8h; these results directly impact on the number of equivalent hours which are higher for the two low temperature cases. The resulting economic analysis is encouraging, showing comparable LCOE for the innovative mixture and for sCO_2 cycles. Moreover, considering the economies of scale that intrinsically characterize the cost function [16], a further LCOE reduction may be expected for larger solar field and increased power block sizes.

Sensitivity Analysis on the Equation of State for the CO_2+C_6F_6 Mixture

The volumetric and thermodynamic behavior of CO_2-based mixtures is not yet fully described in literature, thus the selection of the most proper equation of state is not trivial. The same analysis carried out in the previous chapter is performed using the aforementioned PR-BM EoS. Key results are presented in Table 3, showing a non-negligible discrepancy both on efficiency and on LCOE. Further experimental data for the EoS calibration will thus be needed.

TABLE 3. Effect of the EoS variation on the thermodynamic and economic performances of the CO_2+C_6F_6 cycle

	PR-BM	PR
Cycle efficiency at T_{max} = 550°C [%]	41.1	42.5
Cycle efficiency at T_{max} = 650°C [%]	45.1	46.4
LCOE at T_{max} = 550°C [$/MWh]	139	132
LCOE at T_{max} = 650°C [$/MWh]	165	159

Comparison with Conventional Steam Rankine Cycles

Finally, a comparison with a conventional steam cycle for the commercially available technology exploiting solar salts as HTF is proposed: the steam cycle characteristics are consistent with the reference literature for this solar field [16] and the economic assumptions of this work. The optimal TES size for the LCOE was also computed and fixed at 10h. Nevertheless, the steam cycle efficiency is lower than the ones of the sCO_2 and CO_2+C_6F_6 cycles, and therefore its yearly net energy produced is also lower.

Table 4 shows the CAPEX breakdown and the net energy produced, along with the resulting LCOEs: the total CAPEX results in similar values between the three configurations considering the same percentage of indirect and contingency costs. The most significant difference between the conventional and the two innovative technologies is the actual energy production along the year: for this reason, a clear reduction of the LCOE of CO_2+C_6F_6 cycle with respect to steam Rankine cycles occurs. A more conservative approach may consider a different percentage of indirect and contingency costs as function of the technological maturity of the different solutions as in [16], thus reducing the advantages of sCO_2 and sCO_2-C_6F_6 cycles.

TABLE 4. Results for the Steam Rankine cycle, the sCO_2 and CO_2+C_6F_6 cycles for T_{max}=550°C

	Steam Rankine Cycle	**sCO_2 Cycle**	**CO_2+C_6F_6 Cycle**
Heliostat field [M$]	40.8	40.8	40.8
Solar Tower + Receiver [M$]	52.7	52.7	52.7
Storage [M$]	17.9	25	23.5
Power Block [M$]	44.5	40.1	37.4
Indirect + Contingency Costs [M$]	31.2	31.8	30.9
Total CAPEX [M$]	187.1	190.6	185.3
Power Block specific costs [$/kWel]	1400	1176	1106
Power Plant specific costs [$/kWel]	6134	6015	5830
TES [h]	10	8	8
Yearly Net Energy Produced [GWh]	140.9	149	149.4
Equivalent Hours [h/year]	4619	4700	4698
LCOE [$/MWh]	141	135	132

CONCLUSIONS

The proposed work compares conventional Rankine cycles, sCO_2 and transcritical CO_2 mixture (CO_2+C_6F_6) cycles with the same solar field, receiver, location, and cost assumptions. The adopted cost functions for conventional TES, solar tower and heliostat field represent the current component costs, higher than the ones usually proposed in literature, which are often target costs. The economic analysis underlines interesting results for the innovative working fluid, showing potentialities to reduce the power block CAPEX and the LCOE with respect to sCO_2 technology. The obtained results are significantly affected by the adopted equation of state to model the mixture, indicating the necessity of more accurate experimental data for the morel calibration.

ACKNOWLEDGMENTS

This paper is part of the SCARABEUS project that has received funding from the European Union's Horizon 2020 research and innovation programme under grant agreement No 814985.

REFERENCES

1. "sCO2-flex - sCO2flex," n.d. https://www.sco2-flex.eu/.
2. Crespi F, Sánchez D, Rodríguez JM, Gavagnin G. "A thermo-economic methodology to select sCO2 power cycles for CSP applications." *Renew Energy* 147 (2020): pp. 2905–2912. https://doi.org/10.1016/j.renene.2018.08.023.
3. Scarabeusproject n.d. https://www.scarabeusproject.eu/.
4. Dias AMA, Daridon JL, Pa JC. "Vapor - Liquid Equilibrium of Carbon Dioxide - Perfluoroalkane Mixtures : Experimental Data and SAFT Modeling." *Ind Eng Chem Res* 45 (2006): pp. 2341-2350.
5. "Aspen Plus | Leading Process Simulation Software | AspenTech." n.d. https://www.aspentech.com/en/products/engineering/aspen-plus.
6. Mehos M, Turchi C, Vidal J, Wagner M, Ma Z, Ho C, et al. "Concentrating Solar Power Gen3 Demonstration Roadmap." Nrel/Tp-5500-67464 (2017): pp. 1-140. https://doi.org/10.2172/1338899.
7. "Solar Power Tower Integrated Layout and Optimization Tool | Concentrating Solar Power | NREL." n.d. https://www.nrel.gov/csp/solarpilot.html.

8. Pacio J, Singer C, Wetzel T, Uhlig R. "Thermodynamic evaluation of liquid metals as heat transfer fluids in concentrated solar power plants." *Appl Therm Eng* 60 (2013): pp. 295-302. https://doi.org/10.1016/j.applthermaleng.2013.07.010.
9. Binotti M, Invernizzi CM, Iora P, Manzolini G. "Dinitrogen tetroxide and carbon dioxide mixtures as working fluids in solar tower plants." *Sol Energy* 181 (2019): pp. 203-213. https://doi.org/10.1016/j.solener.2019.01.079.
10. Polimeni S, Binotti M, Moretti L, Manzolini G. "Comparison of sodium and KCl-MgCl2 as heat transfer fluids in CSP solar tower with sCO2 power cycles." *Sol Energy* 162 (2018): pp. 510-524. https://doi.org/10.1016/j.solener.2018.01.046.
11. Binotti M, Astolfi M, Campanari S, Manzolini G, Silva P. "Preliminary assessment of sCO2 cycles for power generation in CSP solar tower plants." *Appl Energy* 204 (2017): pp. 1007-1017. https://doi.org/10.1016/j.apenergy.2017.05.121.
12. Jonemann M. *Advanced Thermal Storage System with Novel Molten Salt.* 1979.
13. Weiland NT, Lance BW, Pidaparti SR. "SCO2 power cycle component cost correlations from DOE data spanning multiple scales and applications." *Proc. ASME Turbo Expo* 9, American Society of Mechanical Engineers (ASME); 2019. https://doi.org/10.1115/GT2019-90493.
14. Carlson MD, Middleton BM, Ho CK. "Cycles Using Component Cost Models Baselined With Vendor Data." *Proc ASME 2017 Power Energy Conf* 2017: pp. 1-7.
15. "AACE International recommended Practice. Cost-Estimate classification system - as applied in Engineering procurement and construction for the process industry." 2018.
16. Manzolini G, Binotti M, Bonalumi D, Invernizzi C, Iora P. "CO2 mixtures as innovative working fluid in power cycles applied to solar plants. Techno-economic assessment." *Sol Energy* 181 (2019): pp. 530-544. https://doi.org/10.1016/j.solener.2019.01.015.
17. Laube T, Marocco L, Niedermeier K, Pacio J, Wetzel T. "Thermodynamic Analysis of High-Temperature Energy Storage Concepts Based on Liquid Metal Technology." *Energy Technol* 8 (2020): 1900908. https://doi.org/10.1002/ente.201900908.